

Evidence for and relationship between recent distributed extension and halokinesis in the Farasan Islands, southern Red Sea, Saudi Arabia

Khalid A. Almalki · Laurent Ailleres · Peter G. Betts ·
Rashad A. Bantan

Received: 15 March 2014 / Accepted: 20 January 2015 / Published online: 4 February 2015
© Saudi Society for Geosciences 2015

Abstract This paper presents a structural evolution study of the Farasan Bank using an integration of field work, remote sensing data, and regional Bouguer gravity data interpretation. The architecture of the Farasan Islands is influenced by normal faults parallel to the Red Sea rift axis delineating a series of graben and asymmetric half-graben structures as well as salt domes. Geological data suggest that the negative gravity anomaly over the Farasan Bank reflects thick salt deposits. The gravity data shows a general NW-SE trend with the main negative anomaly coincident with the Farasan Islands. Gravity data together with seismic reflection data suggest that salt diapirs are elongated and parallel to the main rift orientation (NW-SE). This indicates that salt deposition and diapirism was controlled by rift-related basement structures. Forward modeling of gravity data constrained by marine seismic reflection interpretation reveals that the evaporites directly overlie the basement in most places. No pre-evaporite formation was detected. Integration of the modeling with field

observations and interpretations suggests that the Farasan Islands are in an area of active extension. Extension and salt diapirism on the flank of the mid-ocean ridge is likely to be synchronous with renewed spreading at 5 Ma.

Keywords Farasan · Red Sea · Salt diapirism · Remote sensing · Gravity

Introduction

The Farasan Islands are located at the south eastern end of the Red Sea (Fig. 1a). The two main islands, Farasan Alkabir and Sajid, trend parallel to the Red Sea in a northwest to southeast direction. The larger of the two islands, Farasan Alkabir, is approximately 60 km long and is 5 to 10 km wide. Sajid is 30 km long and approximately 12 km wide. Sea depths in the area are almost always less than 100 m with depths of a few meters being common (Fig. 1b). The general elevation of the Farasan Islands varies between 10 and 20 m above sea level, with a peak elevation of 70 m at Zifaf Island. The landscape of the islands appears as low brown limestone platforms. The surface of the Farasan Islands and a number of small islets between the main Farasan Island group and the coast consist of an originally near uniform coral reef limestone (Mideast Industries Ltd. 1966; Skipwith 1973; Ministry of Petroleum and Mineral Resources 1986).

K. A. Almalki (✉)
King Abdulaziz City for Science and Technology, PO Box 6086,
Riyadh 11442, Kingdom of Saudi Arabia
e-mail: kmalki99@gmail.com

L. Ailleres · P. G. Betts
School of Geosciences, Monash University, PO Box 28E, Wellington
Road, Clayton, VIC 3800, Australia

L. Ailleres
e-mail: Laurent.ailleres@monash.edu

P. G. Betts
e-mail: Peter.Betts@monash.edu

R. A. Bantan
King Abdulaziz University, PO Box 80177, Jeddah, Kingdom of
Saudi Arabia
e-mail: rbantan@kau.edu.sa

Most of the geological and geophysical studies along the Red Sea suggest rifting in the Red Sea initiated at the Late Oligocene ca 30 Ma (Hall 1989; Bosworth et al. 2005); however, the sedimentary record is mainly preserved as evaporitic shelf succession of the Farasan Bank, at the margin of the Arabian Plate, that formed at the beginning of the Miocene ca 22 Ma (Blank et al. 1986; Mandur 2009). The bank contains a lower package of shale and variably thick evaporitic successions up to 4 km thick overlain by Pliocene-Pleistocene limestone (Skipwith 1973; Khalil 2012). The Farasan Bank may record the erosion of the uplifted Arabian continental margin along the southern Red Sea between ca 15 and 5 Ma (Almalki et al. 2014). This is supported by fission track dates from the Arabian Shield which indicate that uplift occurred in the last 14 Ma (Bohannon et al. 1989).

A period of tectonic quiescence ensued in which no extension occurred until the onset of renewed seafloor spreading at ca 5 Ma (Almalki et al. 2014). Spreading is still active today (Ligi et al. 2011). Previous interpretation of the tectonic history of the region regarded the Farasan Bank as being a passive margin (e.g., Dabbagh et al. 1984); however, no attempt was made to explain the development of recent extensional structures within the Farasan Islands.

We combine regional Bouguer gravity data over the bank, high-resolution gravity data over the islands and field structural mapping from the Farasan Islands to illustrate the structural evolution of the bank. Reprocessed, filtered, and forward modeling of the Bouguer gravity data constrained by marine seismic interpretation were used to illustrate the diapiric structures under the Farasan Bank and the southwestern coast of Saudi Arabia. The result shows that the islands are controlled by two patterns of extensional fault activity.

Data and analysis

Processed satellite images together with bathymetric and topographic data were interpreted visually to identify geological structures (Figs. 2 and 3) because they delineate rock boundaries and structures. A structural lineament map of the entire area (Fig. 4) was interpreted from Landsat ETM (15 m resolution: Fig. 1a), SPOT-5 (2.5 m resolution: Fig. 2), and Radarsat (8 m resolution: Fig. 3), which were acquired between 2003 and 2005. Normal faults and domal structures are the most prominent features of the map. These structures were the focus of fieldwork, which involved collecting structural geological data and analysis to constrain our interpretation of remotely sensed imagery.

Fig. 1 a Landsat ETM image (15 m resolution) of the southern Red Sea showing the location of the Farasan Islands, the axial trough, and the gravity survey boundary (in gray) after Gettings (1977, 1983). b Bathymetric and topographic features of the Farasan Bank, the axial trough, and the onshore of southwestern Saudi Arabia after Becker et al. (2009)

Field studies were undertaken between 2009 and 2010 and were the major source of data for the onshore and coastal structural features of the Farasan Islands. The main problem encountered with field mapping was the difficulty of identifying geological features evident from satellite images on the ground, for example, the fault system north of Sajid Island imaged by SPOT-5 (Fig. 2c). This was made particularly difficult because of the low relief of much of the islands.

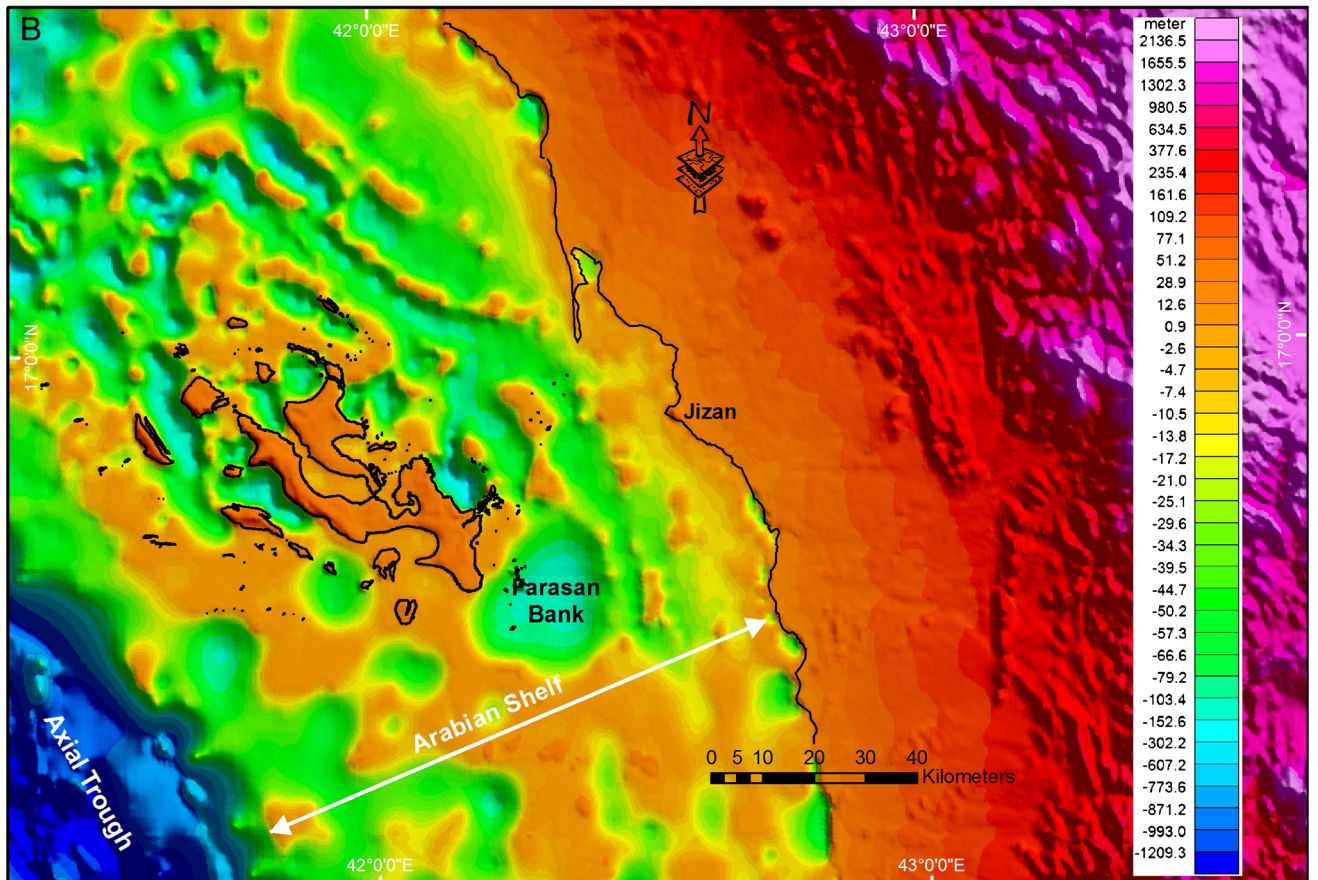
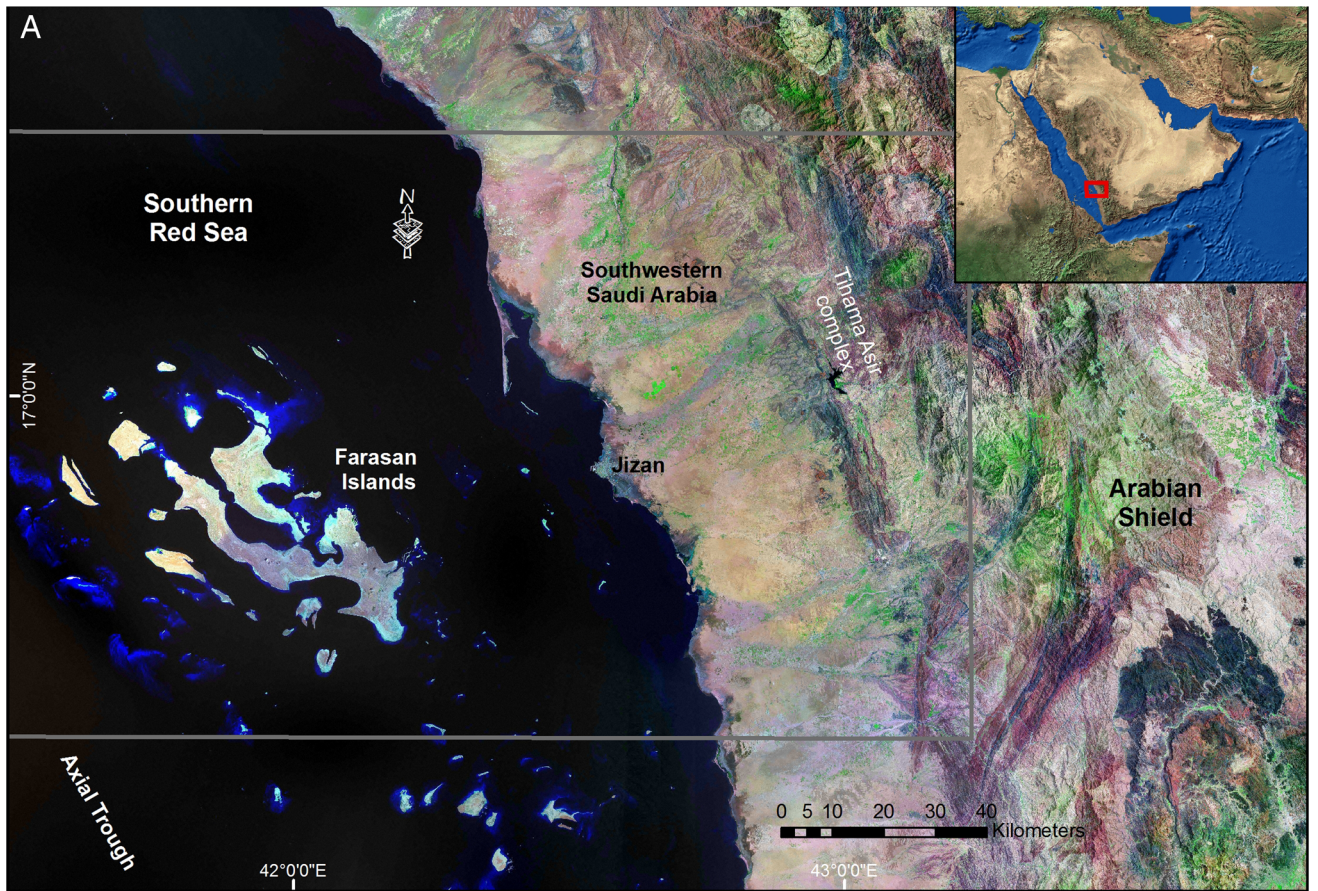
Data from two gravity surveys have been obtained from the Saudi Geological Survey. The first set of data is a complete Bouguer-corrected survey, produced from gravity observations at 145 gravity stations (Gettings 1977, 1983). All stations are at or near sea level. This survey covers a 150×120-km² area extending from the Arabian Shield across the coastal plain and the Farasan Bank to the axial trough of the Red Sea (Fig. 1a). The data were gridded with a grid cell size of 500 m (Fig. 5a). The second data set is a high-resolution Bouguer gravity data set over the islands based on 1216 gravity stations including 19 profiles with a spacing of 50 m (Fig. 6a). Tilt derivative (TDR; Verduzco et al. 2004) filter of the high-resolution gravity anomalies over the islands were used to enhance the geophysical signal of the basement structures under the islands and provide more detail on the distribution of the diapiric structures and associated faults (Fig. 6b).

An interpretative map that shows the geometry of the salt bodies under the bank was attained (Ministry of Petroleum and Mineral Resources 1986). The map (Fig. 5b) was constrained from confidential seismic reflection data and digitized to constrain geophysical modeling.

Satellite image features

Linear ridges

Spectral information for structural lineaments was interpreted by using Landsat infrared bands 4, 5, and 7; SPOT true color images; and Radarsat images with single microwave frequency. Areas clearly defined by linear ridges and faults are shown by their tonal contrast (Fig. 4). These parallel lineaments were examined in the field in the Alhussain and Khilah areas, respectively, in



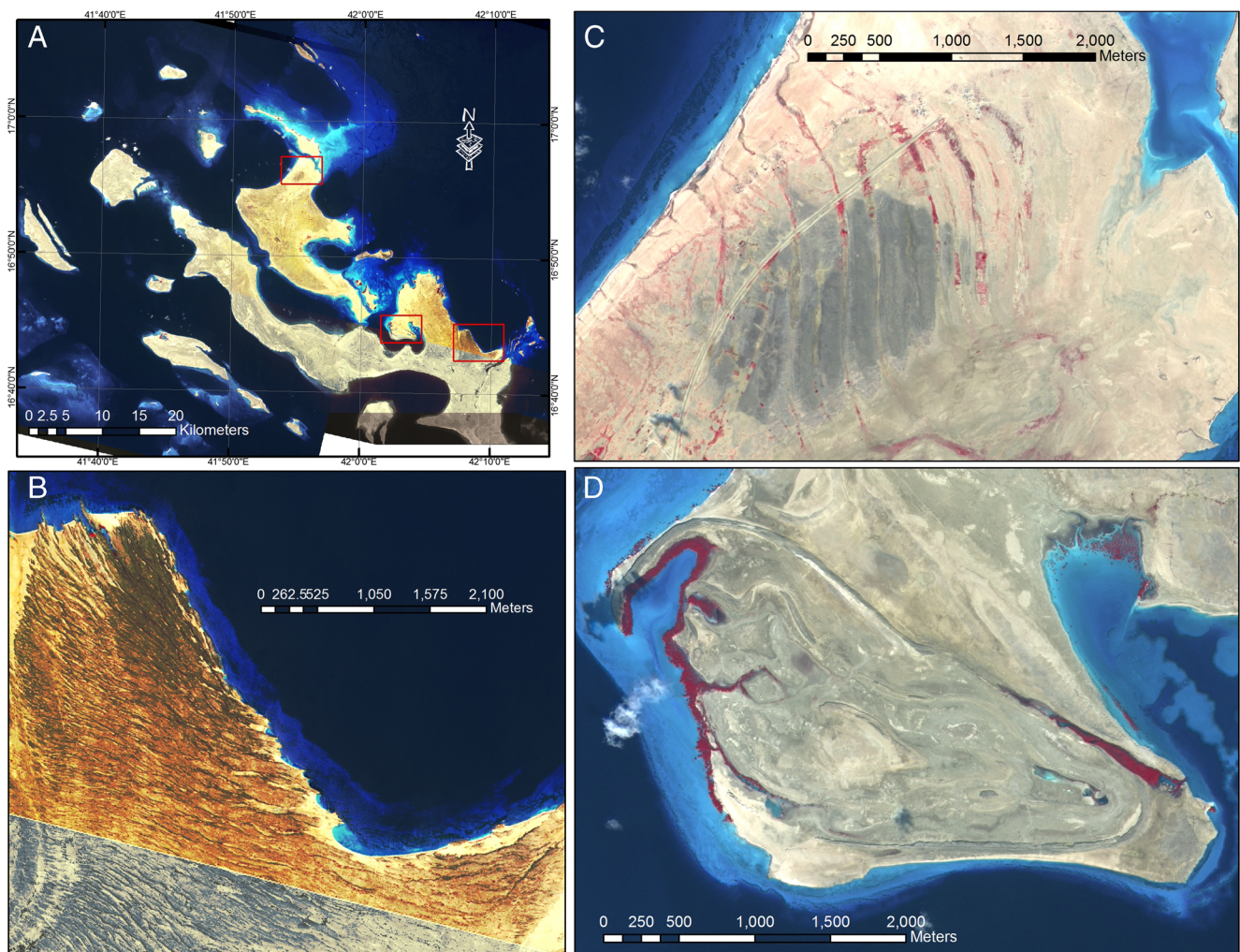


Fig. 2 **a** SPOT-5 images stereo data (2.5 m resolution) of the islands. **b** Khilah fault system trending NW, **c** north of Sajid Island fault layers, and **d** close-up view of Ras Hassis dome structure

the south and northeast of the Farasan Alkabir Island. Most lineaments have a NW-SE trend, which is parallel to the Red Sea axis. However, NE-SW trending lineaments are also evident in the remotely sensed data (e.g., Qumah Island) (Fig. 4).

The configuration of the islands shoals closely parallels the trend of the Red Sea rift system. The satellite images and bathymetric features demonstrate this parallelism (Figs. 1, 2, and 3). The trend of the terrain clearly shows the NW-SE direction of the subbasins and shallows surrounding the islands, as well as the parallel steep slope down to the axial deep trough of the Red Sea (Fig. 1b). As these structures are parallel with the rift axis, we propose that they are likely to have formed in response to active tectonic forces responsible for the motion of the Arabian Plate (McClusky et al. 2010) and seafloor spreading.

Domal structures

The islands are dominated by numerous circular to irregularly shaped diapiric structures as seen on a Radarsat image (Fig. 3). Elongated anticlines (e.g., on Ras Hassis; Fig. 7) are also interpreted. These are interpreted to be caused by rising salt diapirs. They range in size from 3 to 35 km in diameter and vary from circular to elliptical shape in map view. Arcuate faults occurred at the flanks of the diapiric structures or domes (Figs. 4 and 7).

It is evident that the morphology of the coast is affected by diapirism (Fig. 1b). The bathymetric features of the area indicate depression signatures in different places over the Farasan Bank. Figure 1b shows the distinctive occurrence along the coastline of circular or oval bays. A number of these depressions have a NW-SE elongated shape with steep sides and a flat bottom,

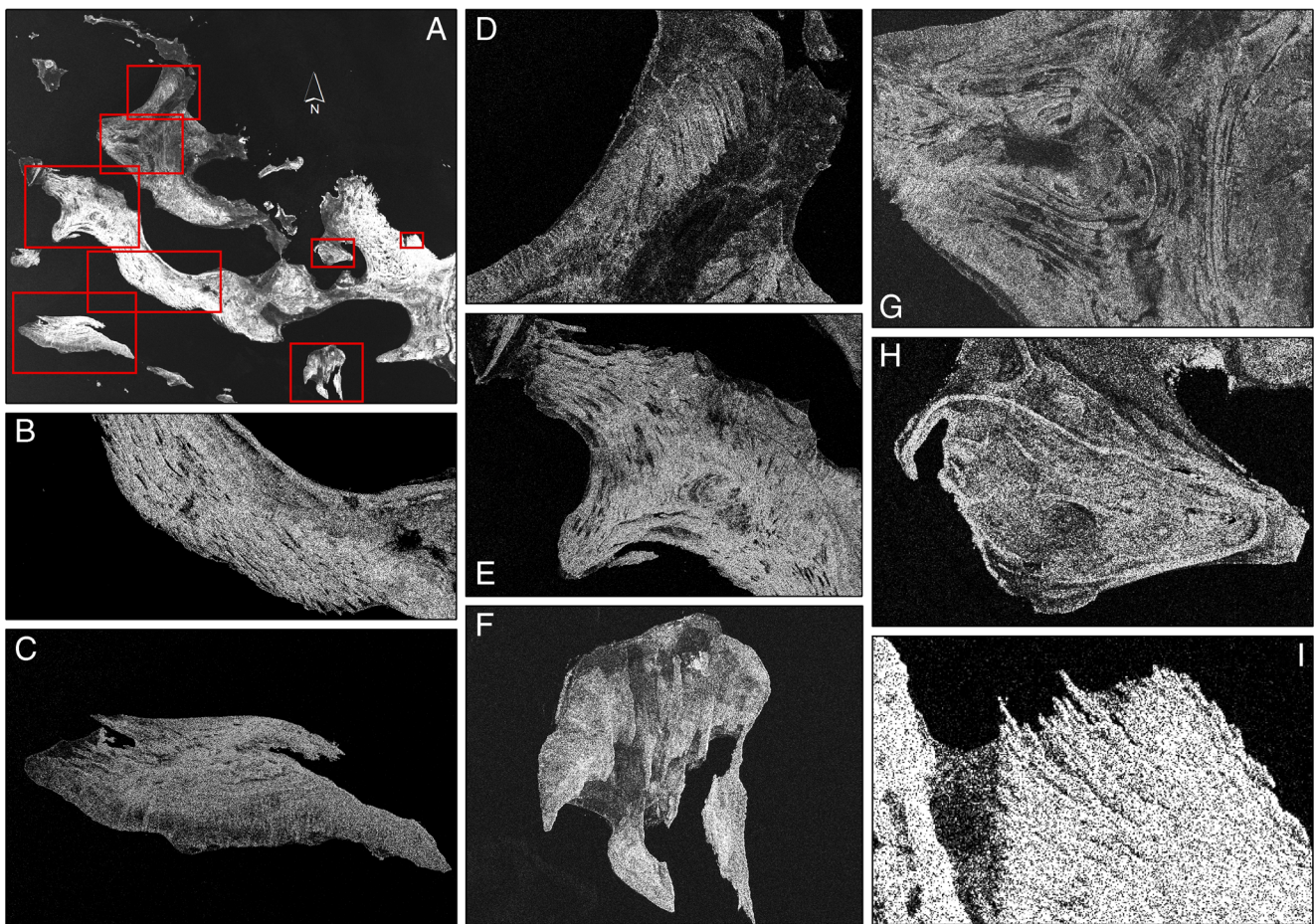


Fig. 3 **a** Radarsat images (8 m resolution). **b** Southwestern Farasan Alkabir fault system trending NW parallel to the Red Sea rift; **c** Zifaf island; **d** faults system detected, northern of Sajid Islands; **e** western

Farasan Alkabir dome structure; **f** Qumah Island faults system trending north; **g** Sajid Island dome structure; **h** Ras Hassis dome structure; and **i** Khilah fault system trending NW parallel to the Red Sea rift

having nearly uniform depths between 5 and 10 m. On the other hand, some of the circular depressions have very steep sides as they reach depths of >200 m. These depressions are likely to be related to buoyancy-driven halokinesis resulting in salt diapirism. However, the halokinesis may have been triggered crust extension at the rift axes or extension within the Farasan Bank, since many of domes appear to mimic the rift structures.

Field observations

Five areas were investigated in the field to ground truth faults and domal structures.

Ras Hassis area, Farasan Alkabir Island

The shape of Ras Hassis is elongated in a NW-SE direction parallel to the Red Sea rift system (Fig. 7a). The

surface expression and earlier drilling results indicate a linear central zone where salt is very close to the surface with the roof of the salt diapir dipping away to the south (Mideast Industries Ltd. 1966; Skipwith 1973). The salt diapir or dome beneath Ras Hassis forms an anticlinal structure with coral limestone dipping away from the dome. Along the hinge of the open anticline structure, there are tensional fractures and normal faults that may have resulted from the diapiric movement of salt (Fig. 7b). Some of these faults have >30 m displacement (e.g., southern part of the Ras Hassis dome). The depression in the central portion of the dome is due to erosion and exhibits almost vertically bedded marls unconformably overlain, at least on the margins of the depression, by shallow dipping reefal limestones.

Fractures trending at about 030° within the coral limestone such as those evident on the NW limb of the Ras Hassis salt dome can reach width of about 2 m. The anticline axial surface at this location has

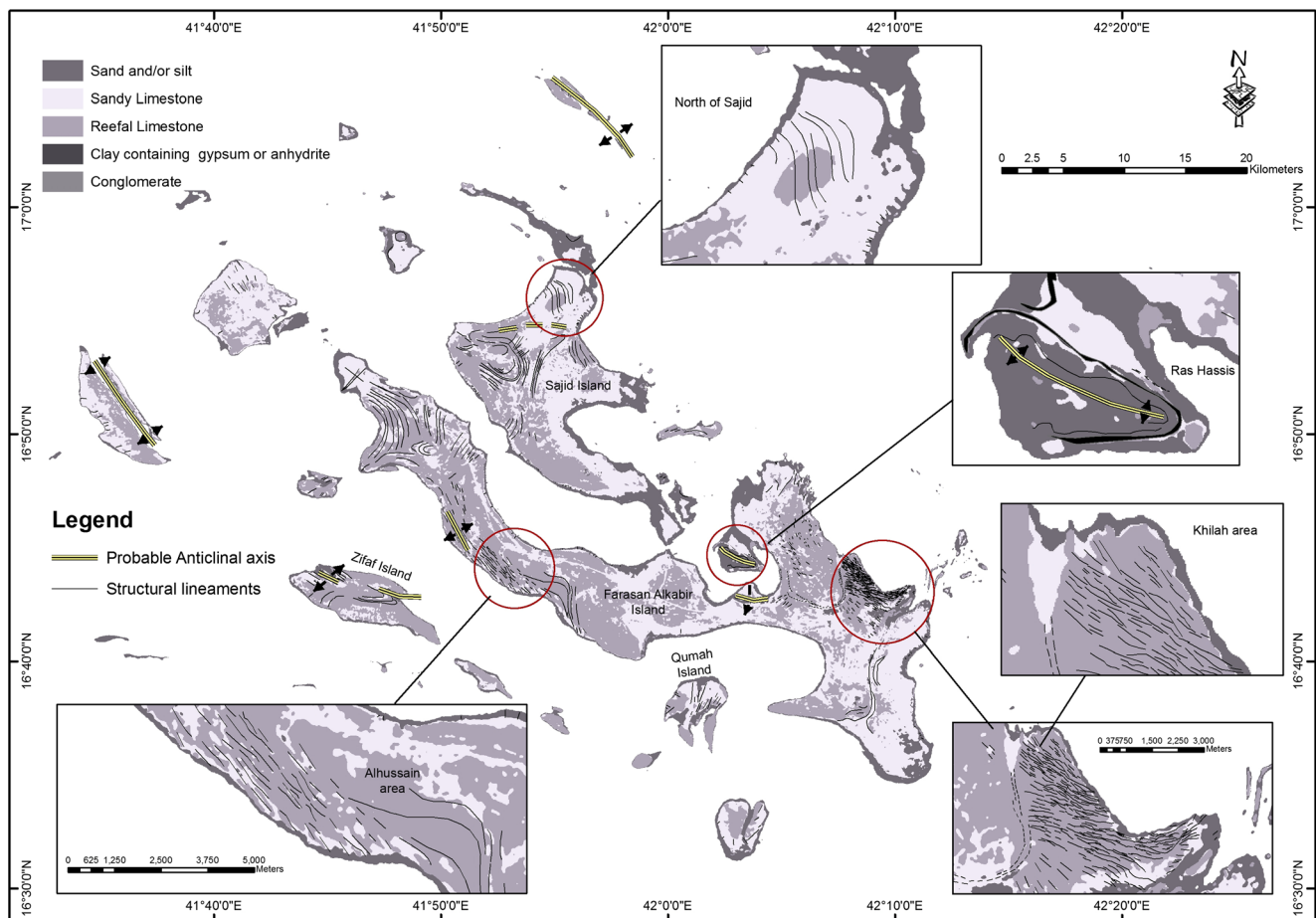


Fig. 4 Structure map of the Farasan Islands interpreted from various satellite images

changed orientation (almost 90° rotation) and appears to envelop the dome (Fig. 7a). In the southern Ras Hassis, major fractures also wrap around the dome and dip to the SW at 74° – 80° . Inside the dome, the fractures and faults are steeply dipping (77° – 85°) to the N-NW direction toward the center of the dome. Fault orientation is variable around the dome, although the majority of the normal faults are parallel to the axis of the Red Sea rift system.

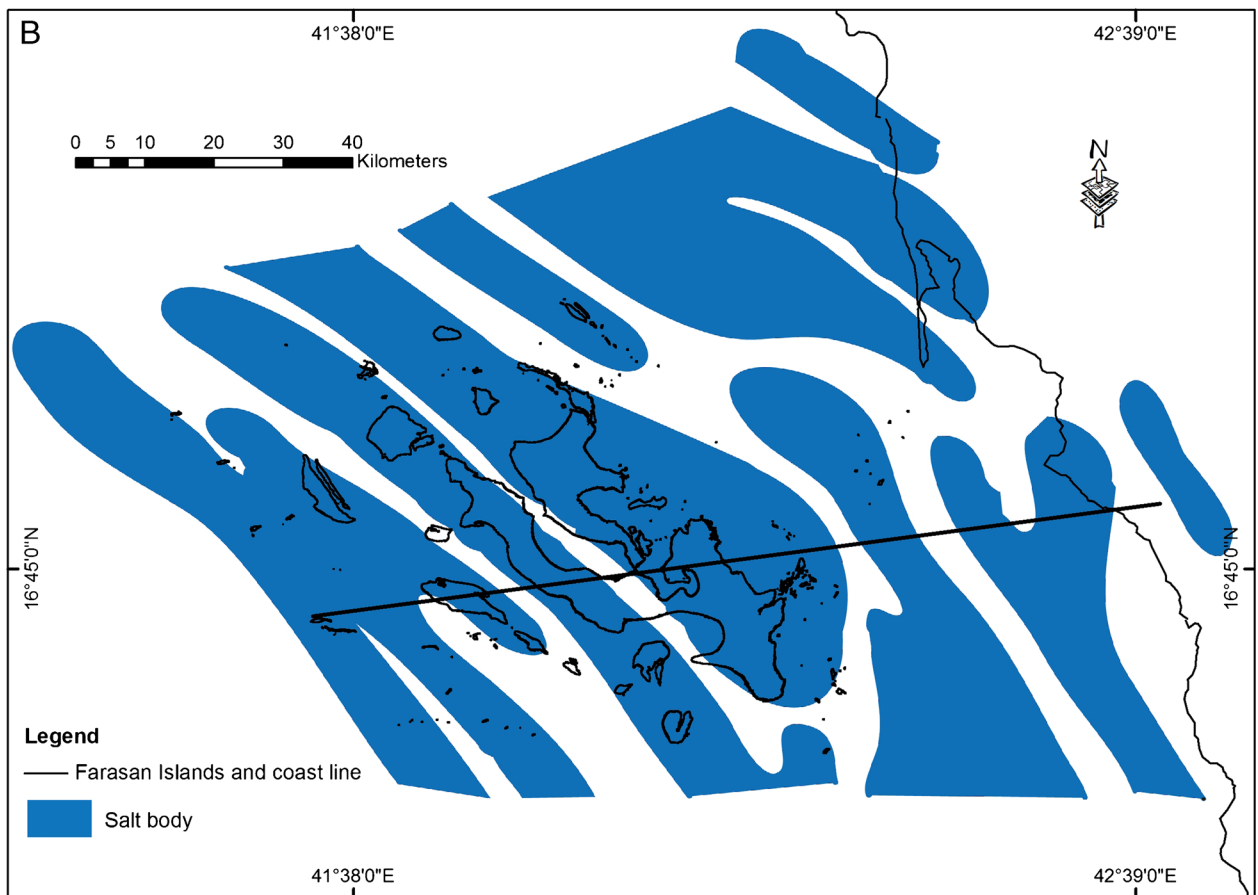
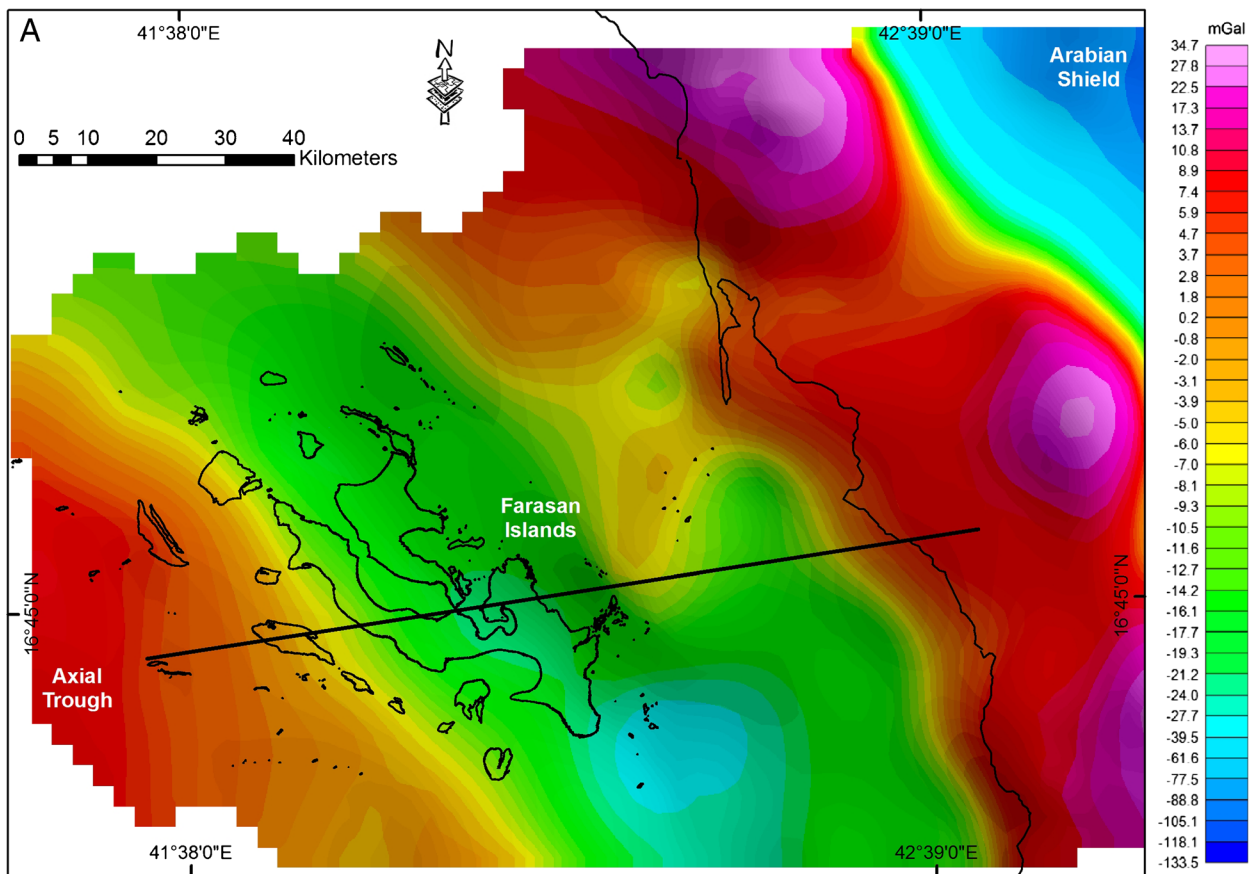
Another spectacular feature of this area is a complex geological relationship within the shale unit which consists of tight folds which are overprinted by several generations of faults (Fig. 7c, d). Bedding in this unit is usually inclined at a low angle, but the rocks are folded and extensively faulted as a result of the Pleistocene and Holocene diapiric movement of salt. Gypsum veins in fractures on the inside margin of the shale beds are also accounting for the severe dome disturbance. Considering the position of the shale on the flank of a diapiric structure, the strike is remarkably constant over the nearly 1-km-long exposure in a NW direction.

Alhussain area, Farasan Alkabir Island

Alhussain area is an area with prominent lineaments with a marked NW-SE trend (Fig. 8). The rocks are extensively faulted. The faults give rise to the linear ridges seen on the SPOT images (Fig. 2). These faults are parallel with the axial trough of the Red Sea. The faults in this area have high angles of dip and are extensional in nature. These faults are the expression of half graben (Fig. 8).

The fault escarpments are well defined as sharp topographic features. Fault scarps are about 3 m high and the hanging wall is usually buried in the sand. The

Fig. 5 a Complete Bouguer gravity data produced from 145 gravity stations and cover the Arabian Shield across the coastal plain and the Farasan Bank to the axial trough of the Red Sea. Grid cell size is 500 m. *White line*: location of profile of Fig. 12. **b** Marine seismic interpretation map showing salt distributions under the bank and the coast of Saudi Arabia modified after Ministry of Petroleum and Mineral Resources (1986). Profile location of Fig. 12 is showing in black



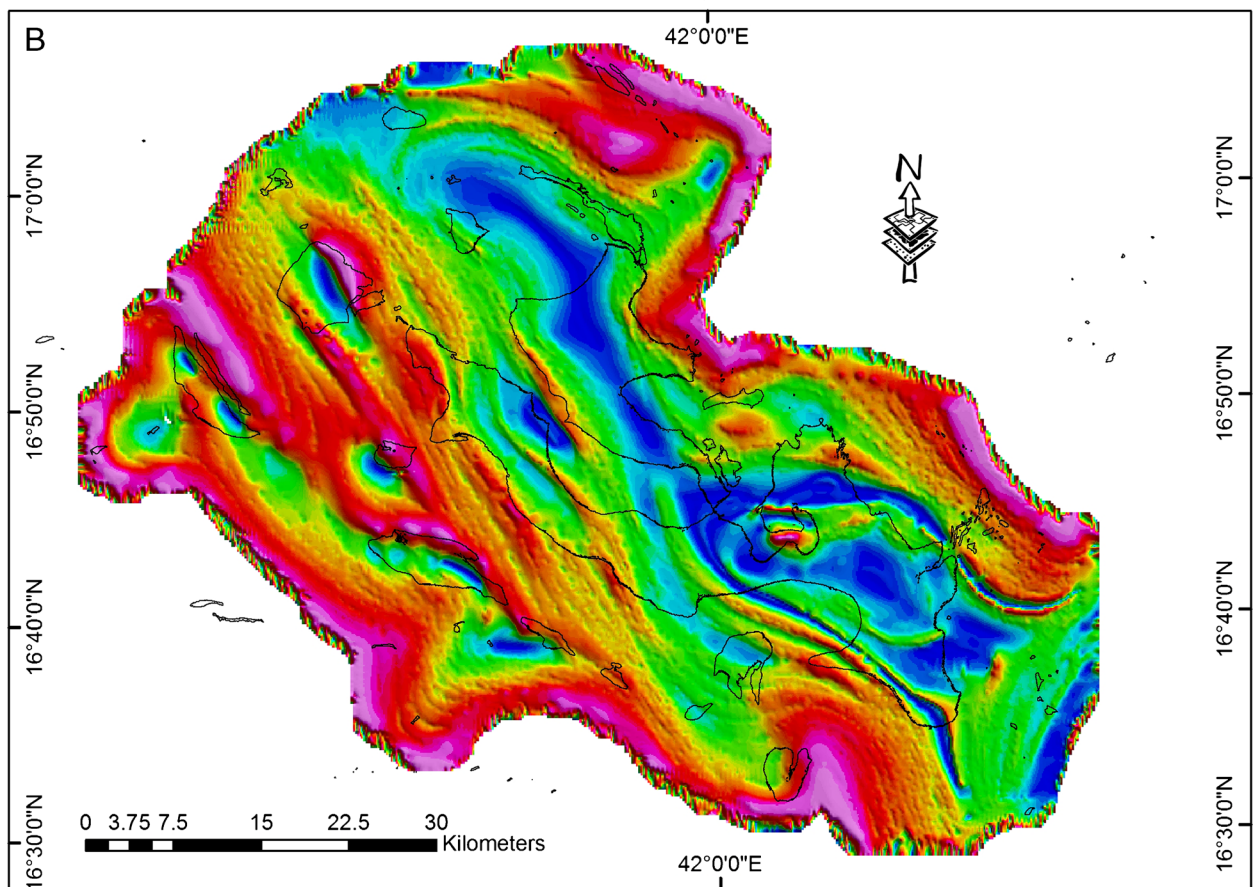
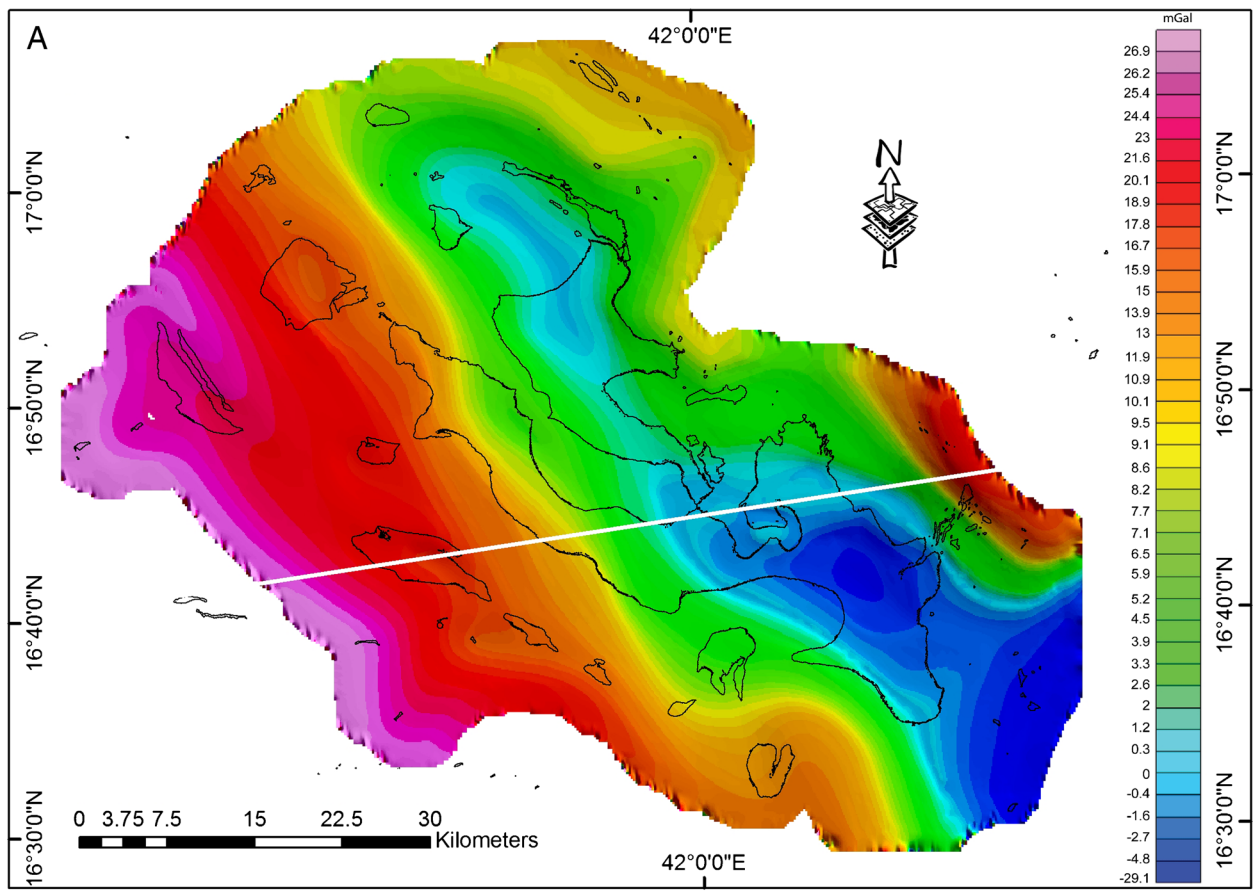


Fig. 6 **a** High-resolution Bouguer gravity data over the islands based on 1216 gravity stations with a spacing of 50 m modified after Ministry of Petroleum and Mineral Resources (1986). Minima in the gravity data are broadly coincident with the dome structures. *White line*: location of profile of Fig. 12. **b** Tilt derivative filter of the Bouguer gravity data showing shallow basement structures. Diapiric anticline forming salt domes with an associated gravity low anomaly. Salt bodies under the islands show trends parallel to the Red Sea rift in a NW direction

majority of the normal faults dip to the NE at 70°. Within the half graben, there are smaller scale fractures. In the normal fault footwall (on the tilt-block crests), most of the bedding dips to the SW at 30°.

Khilah area, Farasan Alkabir Island

The Khilah area in the northeastern part of the Farasan Alkabir Island preserves half graben defining tilt blocks (Fig. 9). Half graben bounding normal faults dip to the NE and N between 50° and 85° (Fig. 9) and trend in

NW-SE direction parallel to the Red Sea rift. Within the tilt blocks, the stratigraphy dips to the SW or S between 10° and 40°. The tilt block crests in the normal fault footwall are defined by limestone ridges. This area has a low relief with fault-related ridges reaching maximum height above sea level of ~20 m.

Sajid Island

Analysis of satellite images (Fig. 4) shows that Sajid Island preserves two major salt domes. A large dome occurs within the central core of the island and is elongated in a NW-SE direction parallel to the Red Sea rift system. A smaller dome in the northern part of the island trends in a NE-SW direction. The domal structures are bound by linear fractures, identified during field investigations, which are oriented in a NW-SE and N-S direction, respectively (Fig. 10). The majority of the fractures dip inward toward the dome.

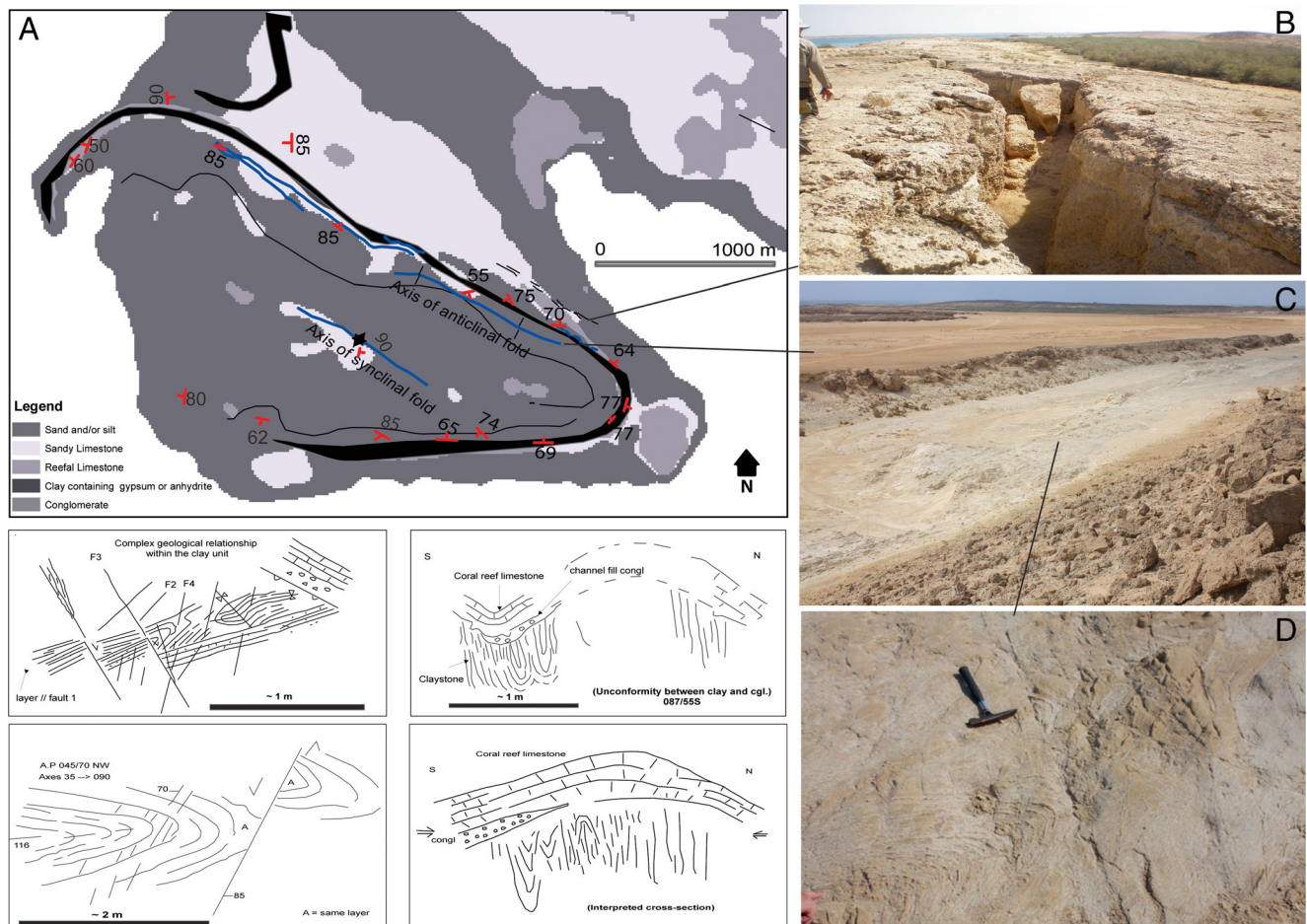


Fig. 7 **a** Field observations from Ras Hassis showing major normal faults (in red) that change orientation around the dome structure. **b** Tensional fractures located along the hinge of the salt dome structure. **c**,

d Shale outcrop. Geological relationship within the shale unit illustrated by cross sections and mapping

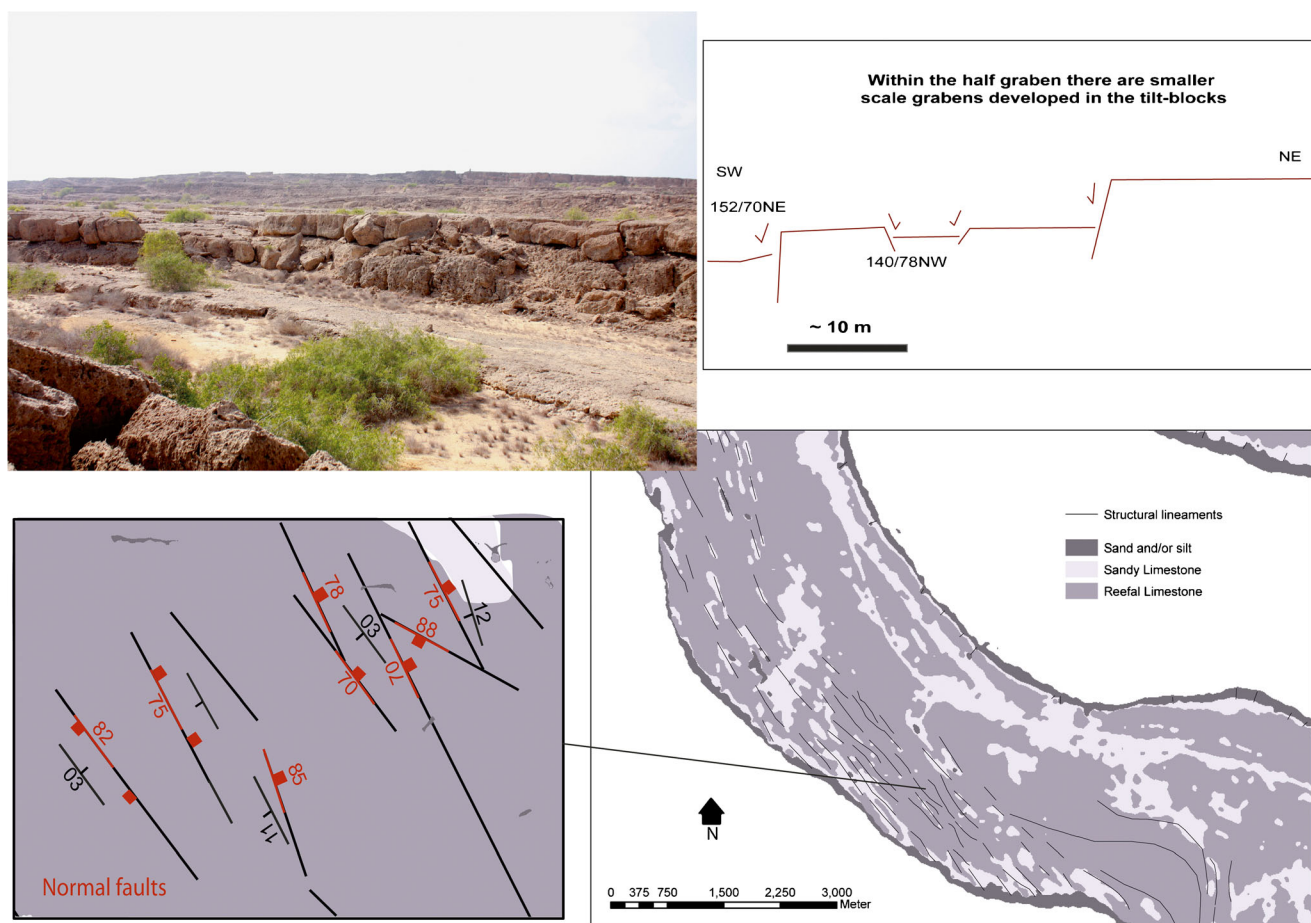


Fig. 8 Alhussain area field observations illustrated by cross section and mapping. Normal faults trending NW, parallel to the rift axis

Three major fractures have been identified from within the northern dome of Sajid Island based on the satellite imagery at $\sim 110^\circ$ to one another (Figs. 2c, 4, and 10). The fracture systems propagate from the central part of the dome, which is surrounded by highly arcuate “ring” faults. The core of the dome remains relatively undeformed and has subsided to form a depression relative to the upthrown flanks. The downthrown central portion exhibits an ellipsoidal geometry which is surrounded by curvilinear faults (Fig. 10). Faults are low-angle faults, with dips between 5° and 7° to the SW in the southern flank and between 7° and 9° to the NE in the northern flank.

The flat elliptical topography in the core of the dome is believed to be the remnants of the salt dome in the central portion of Sajid Island. Several exposures of bedded limestone and mudstone are exposed (Fig. 10). These beds dip between 10° and 20° away from the dome core. Beds are overprinted by fractures that trend at $\sim 110^\circ$. Fractures near the internal part of the dome

and to the east are discontinuous and trend variably at $\sim 60^\circ$. Where exposed, they are typically ~ 10 – 20 cm wide. Closest to the dome core, in the southwest, normal faults are oriented at 040° with steep dips to the SW. Generally, the normal faults trend parallel to the elongated shape of the salt dome. In addition, normal faults bounding tilt blocks also occur near the southwestern coast of Sajid Island (Fig. 10).

Qumah Island

In addition to the primary direction (NW-SE) of most of the structures on the islands, a NE-SW trending fault system occurs on Qumah Island (Figs. 4 and 11). These faults appear to control the shape of the island. Normal faults on the island dip to the NW or the SE between 50° and 80° and likely to bound small graben (Fig. 11). The normal faults vary in strike between 015° and 045° . Crosscutting fractures trending 100° have no vertical displacement and these are located on the shoreline cliffs suggesting that they are joints.

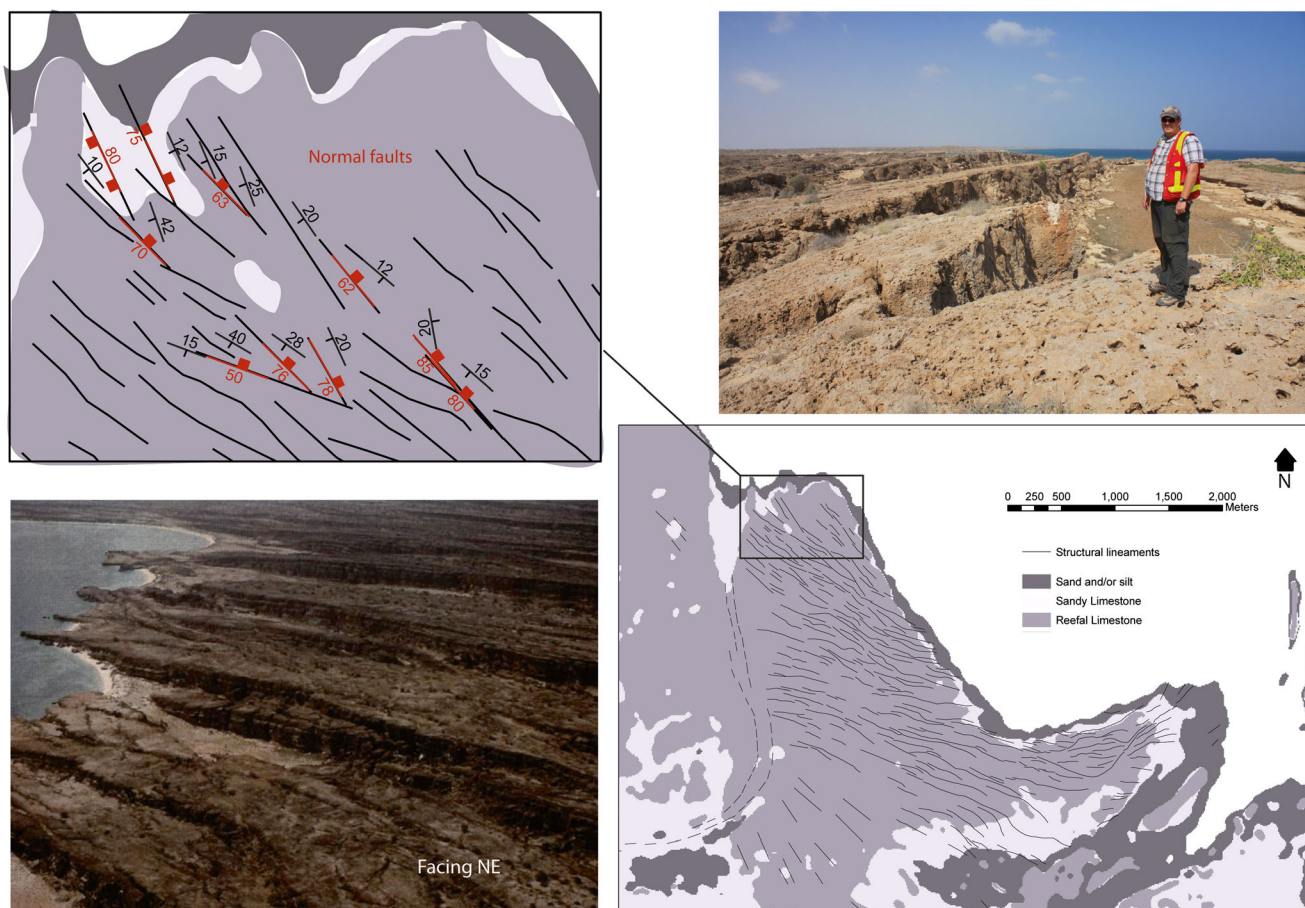


Fig. 9 Khilah observations and selected field picture showing tilt blocks defining half graben. Extensional normal faults parallel to the Red Sea rift dipping NE at angles of between 50° and 85°. Within the blocks, the stratigraphy is dipping to SW or S at angles of between 10° and 40°

Geophysical observations

Previous studies of the Bouguer gravity data (Fig. 5a) have shown that negative anomalies below the Farasan Bank are caused by low-density rocks that correspond with evaporitic rocks intersected by shallow drilling (Mideast Industries Ltd. 1966; Gettings 1977, 1983). Gravity data (Figs. 5a and 6) and marine seismic data (Fig. 5b) appear to image a series of diapiric anticlines resulting from halokinesis. These domes are spatially associated with gravity low anomaly (−30 to 0 mGal).

Interpretation of detailed Bouguer gravity data (Fig. 6) from the Farasan Islands confirms the overall structural pattern derived from field mapping with minima in the Bouguer gravity data broadly coincident with the dome structures. Negative Bouguer values of −30 mGal occur in the southeast Farasan Island and −10 to −25 mGal in an elongated low over the Farasan Islands extending southeastward to the coastal

plain (Fig. 5a). The salt bodies under the islands show trends parallel to the rift axis in a NW direction, possibly implying that salt deposition was controlled by earlier rift structures. The tilt derivative helped identify shallow basement structures (Fig. 6b). On Farasan Alkabr Island, the prolongation of individual structures or domes such as Ras Hassis area is very well expressed (Fig. 6b).

Modeling

On the basis of gravity, bathymetric, and well data constrained by seismic reflection interpretations, a geological cross section has been modeled to illustrate and test the structure of the bank and the upper crust (Fig. 12). The shelf is modeled as a thick, 3000–5000-m sequence of sediments: the evaporite deposits making up about two thirds of the thickness which is consistent with borehole observations. The salt body is modeled with a density of 2.15 g/cm³, while 2.4 g/cm³ was

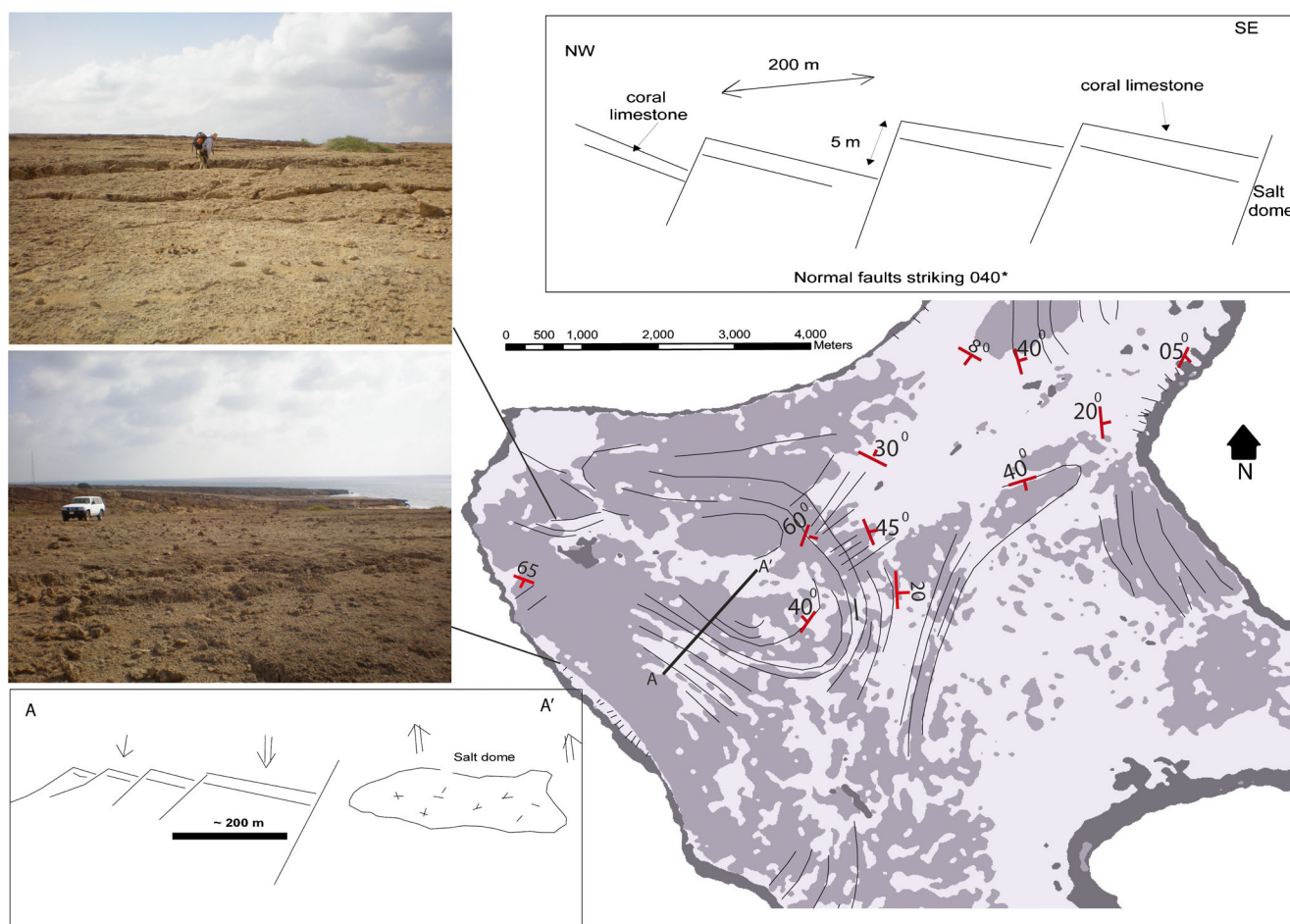


Fig. 10 Sajid cross sections and mapping. Sajid dome elongated in a NW-SE direction parallel to the Red Sea rift system bounded by linear features oriented NW-SE and N-S. Central portion exhibits an ellipsoidal

geometry which is surrounded by curvilinear faults. Normal faults bounding tilt blocks in the southwestern coast of Sajid Island parallel to the Red Sea rift

assigned to the carbonate rocks. The salt bodies have a great influence on gravity modeling.

The model predicts basement depths ranging from 1.5 to 4.5 km below sea level over a distance of 140 km under the bank. This is consistent with well data from the coast of Saudi Arabia (Ministry of Petroleum and Mineral Resources 1986). Under the bank, the offshore basement structures are modeled as a series of half graben, graben, and horsts striking parallel to the rift axis. In the model, the basement rises toward the west approaching the axial trough.

Along the modeled profile (Fig. 12), we modeled eight individual salt domes constrained from seismic reflection interpretation (Fig. 5b) and very short wavelength low-gravity anomalies, which are hardly visible on Fig. 12. However, while the basement geometry is responsible for the very long (width of the section) and mid-length (~1/4 the length of the section) gravity anomalies, a better fit is obtained when adding the salt

domes to model the very short wavelength anomalies. In the model, limestone and evaporite successions cover the entire shelf and extend beneath the coastal region. In addition, the modeled section illustrates a vast and variable thickness variation of salt bodies. Evaporite succession rapidly thickens eastwards from almost zero into a series of swells ~2–4 km thick between the coast and the axial trough. In this model, the Farasan Alkibir Island is a cap to a large salt diapir that is more than 4 km thick. To the west of Farasan Alkibir, another diapiric swell of ~3 km occurs beneath Zifaf Island.

Discussion and conclusion

Remote sensing, field mapping, and geophysical data interpretation were used and integrated to propose a new understanding of the architecture of the Farasan

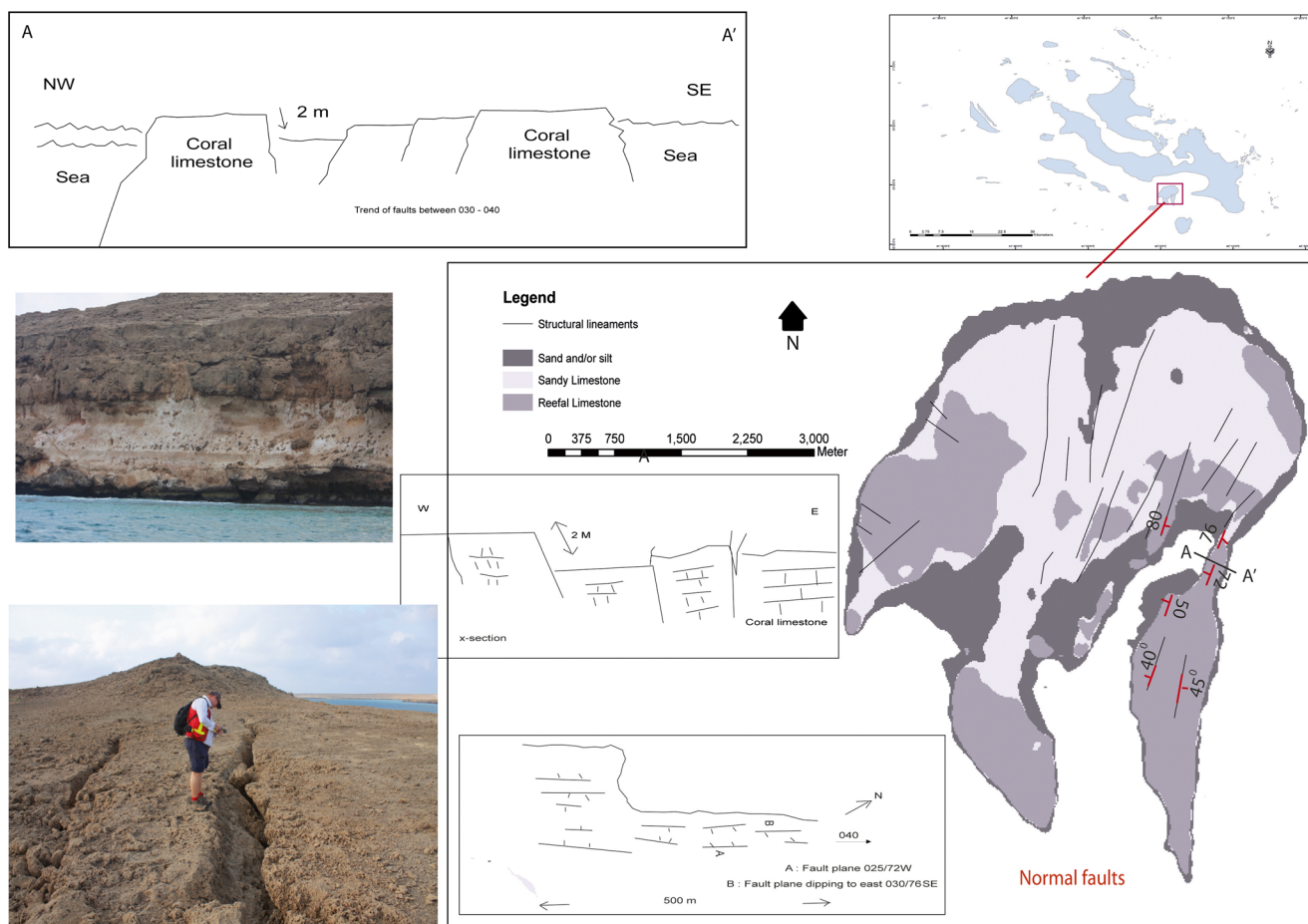


Fig. 11 Qumah Island cross sections and mapping. Normal faults trending NE-SW bound graben structures

Islands and its evolution. Two types of structures were identified in the islands and they include faults and domes, which are at least partially related to salt deformation. Contrasting petrophysical properties (essentially densities) between moderately and relatively dense limestone packages underlying low-density syn-rift evaporites allows for the forward modeling of Bouguer gravity data across the Farasan Bank, especially the short wavelength gravity anomalies.

The islands are dominated by two patterns of extensional fault activity: (1) salt diapirs or domes sourced from Miocene evaporites have resulted in salt doming with elongate geometries parallel or orthogonal to the axis of the Red Sea rift axis. Resultant salt diapirs or domes are bounded by highly arcuate normal faults which sometimes do not extend past the mapped salt accumulation; and (2) limestone coral reefs (<1 Ma) are overprinted by a series of half graben that define a series of tilt blocks that parallel the axis of the Red Sea. In addition, transverse extensional faults in a NE direction were observed on Qumah Island.

Salt diapirs and domes appear to parallel the NW-SE orientation of the Red Sea. We interpret this to be caused by a combination of original depositional architecture of the salt deposits during opening of the Red Sea, as well as reactivation of syn-extensional faults that initially controlled the spatial distribution throughout the Farasan Bank. Diapirism and extension on the flank of the spreading ridge is likely to be synchronous with recent seafloor spreading (ca 5 Ma). Uplift and attenuation of the Farasan Islands through crustal extension is likely to have triggered salt diapirism because there is no conclusive evidence for erosion or differential loading to trigger halokinesis. We do not discuss the occurrence of dissolution and dissolution-related structures as there was no evidence for it in the field. However, dissolution must have affected the volume of evaporites in the Farasan Bank, but its effect on geometries appears to be negligible.

While much of the relative plate motion between Arabia and Africa is taken by the mid-ocean ridge spreading (5–0 Ma), it is evident that extensional fault development within

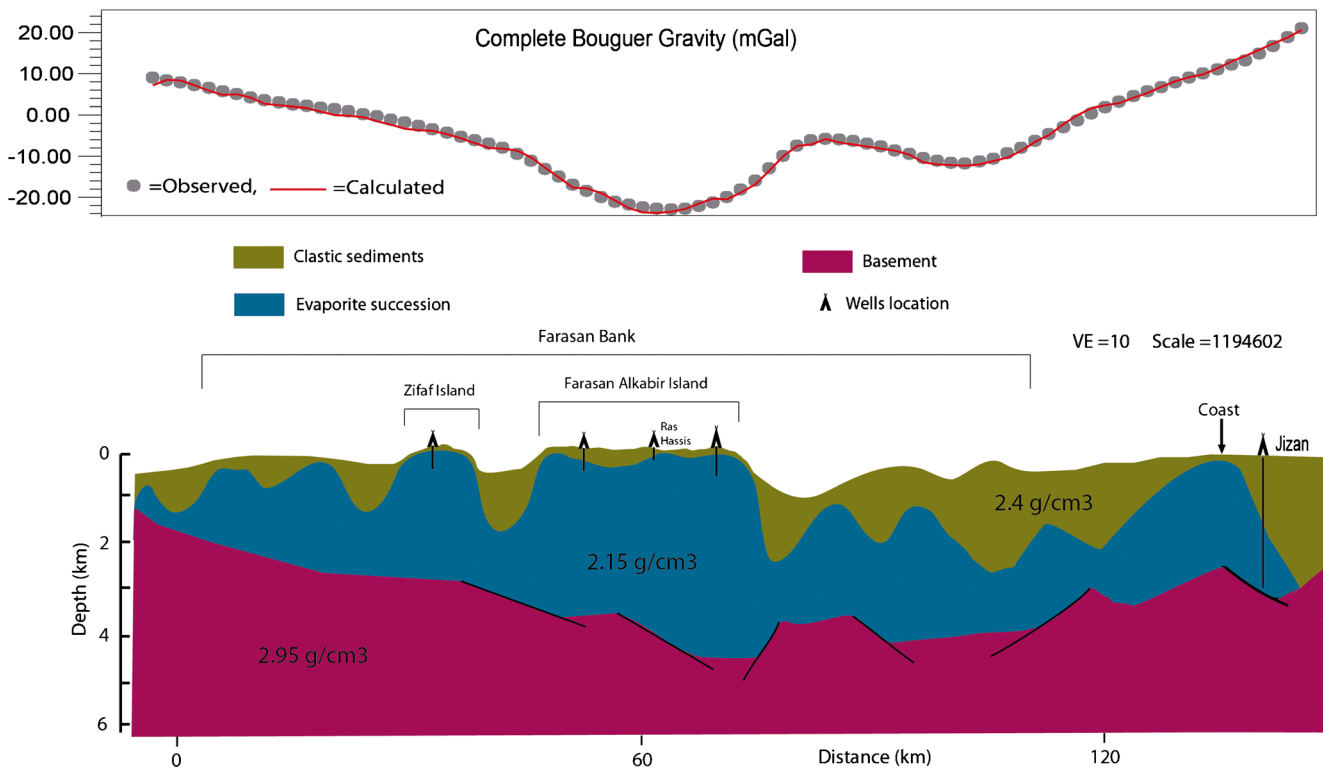


Fig. 12 Forward model of the gravity anomalies over the Farasan Bank (refer to Fig. 5a for profile location). The section was constrained by drilling intersection and seismic reflection interpretation map (Fig. 5b). It should be noted that none of the wells reach the basement

the reefs away from salt accumulation in the Farasan Island must be accommodating some of this plate motion and crustal extension.

Acknowledgments We would like to acknowledge King Abdulaziz City for Science and Technology for financial support for Khalid Almalki and for providing the satellite images. The Geological Survey of Saudi Arabia is thanked for providing geophysical data. Peter Betts is funded by the Monash Research Accelerator Program. Sincere thanks are due to Eng. Hashem Esmael for his valuable support.

References

- Almalki KA, Betts PG, Ailleres L (2014) Episodic sea-floor spreading in the Southern Red Sea. *Tectonophysics* 617:140–149
- Becker JJ et al (2009) Global bathymetry and elevation data at 30 arc seconds resolution: SRTM30_PLUS. *Mar Geod* 32:355–371
- Blank HR, Johnson PR, Getting ME and Simmons, GC (1986) Geologic map of the Jizan Quadrangle Sheet. Kingdom of Saudi Arabia, Ministry of Petroleum, Directorate General of Mineral Resources, 16F, p 25
- Bohannon RG, Naeser CW, Schmidt DG, Zimmwermann RG (1989) The timing of uplift, volcanism and rifting peripheral to the Red Sea, a case for passive rifting. *J Geophys Res* 94:1683–1701
- Bosworth W, Huchon P, McClay K (2005) The Red Sea and Gulf of Aden Basins. *J Afr Earth Sci* 43:334–378
- Dabbagh A, Hotzl H, Schmier H (1984) Farasan islands. In: Jado AR, Zoetl JG (eds) *Quaternary period in Saudi Arabia*, vol 2. Springer-Verlag, Vienna, pp 212–218
- Gettings ME (1977) Delineation of the continental margin in the southern Red Sea from new gravity evidence. In: Hilpert LS (ed) *Red Sea research 1970–1975*, Bulletin, 22. Saudi Arabian Ministry of Petroleum and Mineral Resources, DGMR, pp K1–K11
- Gettings ME (1983) A simple Bouguer gravity anomaly map of southwestern Saudi Arabia and an initial interpretation. U.S. Geological Survey OF-83-789
- Hall SA (1989) Magnetic evidence for the nature of the crust beneath the southern Red Sea. *J Geophys Res* 94:12,267–12,279
- Khalil HM (2012) Pliocene–Pleistocene stratigraphy and macrofauna of the Farasan Islands, South East Red Sea, Saudi Arabia. *Arab J Geosci* 5:1223–1245
- Ligi M et al (2011) Initial burst of oceanic crust accretion in the Red Sea due to edge-driven mantle convection. *Geology* 39:1019–1022
- Mandur MM (2009) Calcareous nannoplankton biostratigraphy of the Lower and Middle Miocene of the Gulf of Suez, Egypt. *Aust J Basic Appl Sci* 3:2290–2303
- McClusky S et al (2010) Kinematics of the southern Red Sea-Afar Triple junction and implications for plate dynamics. *Geophys Res Lett* 37, L05301
- Mideast Industries Ltd. (1966) Salt production possibilities of the Jizan and Farasan Island area. Directorate General of Mineral Resources, Ministry of Petroleum and Mineral Resources, Jeddah, Saudi Arabia DGMR-279:1–13
- Ministry of Petroleum and Mineral Resources (1986) Red Sea Evaporite Project: executive summary of work between 1399 H and 1406 H. Ministry of Petroleum and Mineral Resources, Saudi Arabia SEL-CR-06-11:1–17
- Skipwith P (1973) The Red Sea and coastal plain of the Kingdom of Saudi Arabia. Directorate General of Mineral Resources, Ministry of Petroleum and Mineral Resources, Jeddah, Saudi Arabia TR-1973-1
- Verdusco B, Fairhead JD, Green CM, MacKenzie C (2004) New insights into magnetic derivatives for structural mapping. *Lead Edge* 23: 116–119